

# Uncertainty-Aware Counterfactual Traffic Signal Control with Predictive Safety and Starvation-Avoidance Constraints Using Vision-Based Sensing

Jayawant Bodagala  
*Independent Researcher*  
 CA, USA  
 jayawantbodagala61@gmail.com

Balaji Bodagala  
*Computer Engineer*  
 ENSISINFO INC  
 CA, USA  
 balaji.bodagala@gmail.com

**Abstract**—Real-world deployment of adaptive traffic signal control, to date, remains limited due to the uncertainty associated with vision-based perception, implicit safety, and non-interpretable control policies learned and validated mainly in simulation. In this paper, we introduce UCATSC, a model-based traffic signal control system that models traffic signal control at an intersection using a stochastic decision process with constraints and under partial observability, taking into account the uncertainty associated with vision-based perception. Unlike reinforcement learning methods that learn to predict safety using reward shaping, UCATSC predicts and enforces hard constraints related to safety and starvation prevention during counterfactual rollouts in belief space. The system is designed to improve traffic delay and emission while preventing safety-critical errors and providing interpretable control policy outputs based on explicit models.

**Index Terms**—Traffic signal control, partial observability, belief-space control, MPC, safety constraints, fairness constraints, vision-based sensing.

© 2026 Jayawant Bodagala, Balaji Bodagala. This work may not be reproduced or distributed without permission.

## I. INTRODUCTION

The effectiveness of operation of signalized intersections is a major contributor to traffic flow efficiency, air quality, and safety at these critical areas of convergence of routes [1]. Despite these areas of convergence forming only a very small portion of the overall road network, they are responsible for a disproportionately large amount of traffic delay as a consequence of signal control and the stop–start nature of vehicle movements as traffic approaches these intersections [2], [3]. Because of this operating pattern, vehicles consume more fuel and emit larger quantities of pollutants precisely at locations where traffic signals regulate movement. Empirical studies have conclusively shown that a significant proportion of urban vehicular emissions occur at or near signalized intersections, where inefficient signal timing induces stop-and-go behavior and increases emissions of carbon dioxide ( $\text{CO}_2$ ), nitrogen oxides ( $\text{NO}_x$ ), carbon monoxide (CO), and particulate matter [4]–[7]. The significance of these emissions extends beyond concerns related to climate change and directly

affects the health and safety of populations living and working near major urban roadways [8], [9]. As a result, improving intersection control has emerged as a high-impact strategy for reducing the environmental footprint of urban transportation systems [10].

Control methods based on reinforcement learning (RL), which continuously optimize signal control actions with respect to performance metrics such as delay, queue length, and throughput, have been widely proposed in the literature [11], [12]. However, similar to most existing control approaches, the majority of reinforcement-learning-based traffic signal control schemes implicitly assume true state observability (TSO). In particular, many existing RL-based controllers rely on highly accurate state information, including precise vehicle counts, queue lengths, or even raw video streams [13], [14]. In real-world deployments—especially in vision-based sensing systems—such an assumption is unrealistic. Visual perception at intersections is inherently uncertain due to occlusions, illumination changes, weather effects, and classification errors [15], [16]. Nevertheless, most reinforcement learning approaches treat sensed inputs as deterministic point estimates, relying on single-value representations of the environment state without explicitly modeling observation uncertainty [17].

Moreover, safety considerations are rarely addressed through explicit constraints in reinforcement-learning-based traffic signal control. Instead, safety is typically incorporated indirectly through reward shaping or conditional action filtering mechanisms [18], [19]. While these approaches may reduce risk in average operating conditions, they cannot guarantee the avoidance of critical failures, such as unsafe phase changes during yellow onset when vehicles remain in the dilemma zone or hazardous interactions with pedestrians [20], [21]. In traffic signal control, phase changes are irreversible; once a phase transition is executed, it cannot be undone [22]. Although learned policies may demonstrate strong performance in simulation or controlled field tests, they often lack interpretability, making it difficult to diagnose failures, attribute causes, or certify behavior under stringent validation requirements [23]. When

failures occur, it is frequently unclear whether the root cause lies in sensing errors, state aliasing, reward mis-specification, or unstable policy updates [24]. This lack of transparency undermines trust among transportation authorities, who require predictable behavior under rare but hazardous conditions, along with clear and defensible justification for every control action [25].

#### A. Contributions

UCATSC: a belief space constrained model predictive control (CS MPC) framework for adaptive traffic signal control under vision uncertainty. The main contributions are:

- **Belief space model predictive control for vision-based traffic signal control:** In the present study, the problem of traffic signal control with vision-based sensing has been cast as a belief space receding horizon optimization problem.
- **Predictive Dilemma Zone Safety Constraints:** A belief space conditioned risk constraint for the dilemma zone has been developed. This constraint dictates the decision for the termination of the phases (start of yellow).
- **Starvation Avoidance Fairness Constraints:** Service age constraints are imposed to restrict the maximum waiting time for the phases.
- **Counterfactual Rollouts in Belief Space:** Candidate phase actions are evaluated using counterfactual belief space rollouts. The action with the least cost is selected.
- **Reduced Aggregate Belief Filter for Real-Time Operation:** A movement-level representation of the belief space has been introduced.
- **Reduced Aggregate Belief Filtering for Real-Time Operation:** Zone-level belief aggregation enables real-time control while achieving a **43% reduction** in the total emission proxy.

## II. RELATED WORK

Research in traffic signal control (TSC) has evolved along several complementary directions, reflecting the need to balance theoretical rigor with practical deployability. One line of work focuses on traditional adaptive control strategies and their relationship to actuated signal control. A second direction emphasizes incremental performance improvements driven by real-world deployment challenges, often resulting in stepwise methodological refinements rather than radical redesigns. A third line concentrates on optimization-based approaches, which frequently build upon established control frameworks instead of fully replacing them. In practice, intersection control systems often combine structured, theory-driven flow models with experience-based adaptive logic aimed at substituting for or enhancing manually crafted signal plans.

An increasingly important body of research addresses the sensing and detection layer that underpins traffic signal control. Early systems relied primarily on inductive loop detectors, but sensing technologies have progressively expanded to include richer modalities such as vision-based detection from video streams and radar-based sensing. Despite these advances, a

persistent mismatch remains between the high-dimensional, uncertain observations produced by modern sensors and the predominantly deterministic control architectures that continue to be employed.

Classical approaches to traffic signal management are dominated by coordinated fixed-time plans, actuated control, and large-scale adaptive systems. Survey work on road traffic control strategies formalizes this landscape and continues to serve as a foundational reference for how signal control is structured at the network level, as well as for the performance metrics—such as delay, queue length, and traffic progression—that have historically guided design decisions [1]. Widely deployed systems such as SCOOT and SCATS represent early and influential implementations of online coordination, dynamically adjusting cycle length, green splits, and offsets based on detector measurements and prevailing traffic conditions.

Another major research direction focuses on real-time optimization techniques that frame signal timing as a dynamic control problem. Systems such as RHODES and OPAC exemplify predictive and optimization-driven approaches to traffic signal control. While these methods are conceptually closer to modern model predictive control (MPC) than to classical actuated logic, they were developed under assumptions of relatively low-dimensional system states and reliable sensor inputs. Extending these approaches to environments dominated by vision-based sensing requires explicitly addressing partial observability and measurement uncertainty as central elements of the control problem, rather than treating them as secondary noise sources.

#### A. Why Reinforcement Learning Breaks in Vision-Based TSC

Reinforcement learning (RL) for TSC usually depends on steady and approximatMarkovian state representation, nearly complete data such as reliable queue lengths or vehicle counts—and learn control policies by optimizing expected cumulative reward. However in the real-world vision based sensing pipelines often deliver incomplete, shifting information because of blocked views, lighting shifts, or errors in detecting vehicles over time. This inconsistency blurs distinct states and alters input patterns, breaking key conditions needed for typical reinforcement methods to work well. Rare but serious situations - vehicles caught hesitating when lights turn yellow, or certain lanes waiting excessively - are especially hard to manage. Standard reward averaging misses these infrequent cases. Designing penalties or constraints to handle them reliably remains challenging, even with structured adjustments. Eventually, trained decision rules struggle with hypothetical reasoning, making them harder to test, verify, or trust when risks are high. Taken together, these flaws point toward a different approach - one that the suggested UCATSC method aims to fulfill.

## III. PROBLEM FORMULATION: TRAFFIC SIGNAL CONTROL UNDER PARTIAL OBSERVABILITY

#### A. System State and Control Actions

Let  $x_t \in \mathcal{X}$  denote the true but unobserved traffic state at time  $t$ , consisting of vehicle positions, velocities, intentions,

and queue occupancies. Let  $u_t \in \mathcal{U}$  denote the control action corresponding to a phase extension, termination, or transition.

Traditional actuated and adaptive controllers implicitly assume that  $x_t$  can be approximated by a deterministic measurement  $\hat{x}_t$  obtained from loop detectors, collapsing the control problem into a deterministic or weakly stochastic scheduling task.

### B. Vision-Based Sensing and the Breakdown of Deterministic State Assumptions

Under camera sensing, the measurement process is stochastic, incomplete, and state-dependent. The controller observes

$$z_t \in \mathcal{Z}, \quad z_t \sim p(z_t | x_t), \quad (1)$$

a noisy, biased, and occlusion-prone observation of the true state.

Most existing vision-based TSC systems perform a deterministic reduction

$$\hat{x}_t = f(z_t), \quad (2)$$

and then apply conventional demand-based control logic, effectively ignoring the observation model  $p(z_t | x_t)$ . This creates a structural inconsistency: the controller optimizes a cost function defined over an assumed deterministic state while operating in a partially observable environment.

Queue evolution under uncertainty is modeled as a stochastic difference equation:

$$Q_{m,t+1} = \max(0, Q_{m,t} + A_{m,t} - S_{m,t}(u_t)), \quad (3)$$

where  $A_{m,t} \sim \text{Poisson}(\lambda_{m,t})$  represents arrivals inferred from vision, and  $S_{m,t}(u_t)$  is the (random) service induced by the chosen phase and saturation flow.

This defines a causal queue transition operator  $\mathcal{T}$  that propagates belief states:

$$b_{t+1} = \mathcal{T}(b_t, u_t), \quad (4)$$

enabling forward simulation under candidate actions.

### C. Counterfactual Phase Rollout and Cost

At each decision epoch, the controller enumerates admissible actions  $u \in \mathcal{U}$  and propagates the belief state forward over a finite horizon  $H$ , yielding predicted belief trajectories  $\hat{b}_{t:t+H}^u$ . The expected cost is:

$$J(u) = \mathbb{E} \left[ \sum_{k=0}^H \left( D(\hat{b}_{t+k}) + \alpha R(\hat{b}_{t+k}) + \beta L(\hat{b}_{t+k}) \right) \right], \quad (5)$$

where  $D$  denotes delay,  $R$  denotes safety risk, and  $L$  denotes a starvation penalty proxy. Crucially, UCATSC minimizes (5) subject to hard constraints.

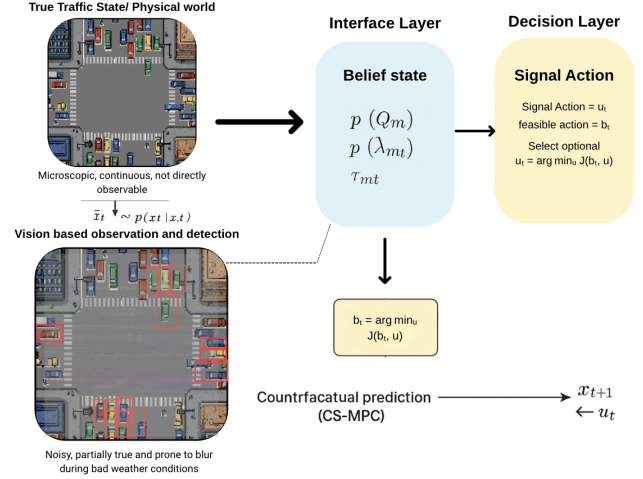


Fig. 1: Vision-based traffic signal control under partial observability. The true microscopic traffic state  $x_t$  evolves via the dynamics model and is observed through a noisy vision measurement  $z_t$ . UCATSC maintains a structured movement-level belief  $b_t = \{p(Q_{m,t}), p(\lambda_{m,t}), \tau_{m,t}\}_{m \in \mathcal{M}}$ , and selects a signal action  $u_t$  via constrained counterfactual rollouts (CS-MPC) subject to predictive safety and starvation-avoidance constraints.

### D. Predictive Safety Constraint (Dilemma Zone Risk)

Let  $(v_i, d_i)$  denote inferred speed and distance of approaching vehicle  $i$ , both uncertain under vision. Define the dilemma-zone risk functional:

$$\mathcal{R}_{\text{DZ}}(b_t) = \mathbb{P}(\text{stop infeasible} \vee \text{clear infeasible} | b_t). \quad (6)$$

A phase transition that initiates yellow is admissible only if

$$\mathcal{R}_{\text{DZ}}(b_t) \leq \epsilon, \quad (7)$$

where  $\epsilon$  is a design threshold.

### E. Fairness via Starvation Barrier Constraint

For each movement  $m \in \mathcal{M}$ , track the service age  $\tau_{m,t}$  and impose:

$$\tau_{m,t} \leq \tau_{\max}, \quad (8)$$

which must hold along all counterfactual rollouts. This guarantees liveness (no indefinite deprioritization).

### F. Belief-Space CS-MPC Problem

At each decision epoch, UCATSC solves a constrained stochastic MPC problem over belief space:

$$u_t^* = \arg \min_{u \in \mathcal{U}} J(u) \quad (9)$$

$$\text{s.t. } \mathcal{R}_{\text{DZ}}(\hat{b}_{t+k}^u) \leq \epsilon, \quad k = 0, \dots, H, \quad (10)$$

$$\tau_{m,t+k} \leq \tau_{\max}, \quad \forall m \in \mathcal{M}, \quad k = 0, \dots, H, \quad (11)$$

plus legal sequencing and minimum green/yellow/all-red constraints.

### G. POMDP Formulation

Vision-based TSC can be formulated as a POMDP. The controller maintains a belief:

$$b_t(x) = p(x_t = x \mid z_{1:t}, u_{1:t-1}), \quad (12)$$

which summarizes available information at time  $t$ . Direct POMDP solutions are intractable at realistic scales; UCATSC uses a reduced, movement-level belief that preserves control-relevant uncertainty.

### H. Belief-State Filtering (Formal)

The vision pipeline produces observations  $z_t \in \mathcal{Z}$  (detections, tracks, class confidences). The true microscopic state  $x_t \in \mathcal{X}$  is not observed directly and evolves as

$$x_{t+1} \sim p(x_{t+1} \mid x_t, u_t). \quad (13)$$

Observations are generated by the measurement model

$$z_t \sim p(z_t \mid x_t). \quad (14)$$

The sufficient statistic for optimal control in a POMDP is the belief

$$b_t(x) \triangleq p(x_t = x \mid z_{1:t}, u_{1:t-1}). \quad (15)$$

The Bayesian filter update is

$$\text{Predict: } \bar{b}_{t+1}(x') = \int p(x' \mid x, u_t) b_t(x) dx, \quad (16)$$

$$\text{Update: } b_{t+1}(x') = \frac{p(z_{t+1} \mid x') \bar{b}_{t+1}(x')}{\int p(z_{t+1} \mid \tilde{x}) \bar{b}_{t+1}(\tilde{x}) d\tilde{x}}. \quad (17)$$

a) *Movement-level reduced belief*.: Direct filtering in  $\mathcal{X}$  is intractable, so UCATSC uses an aggregated movement-level belief

$$b_t \triangleq \left\{ p(Q_{m,t}), p(\lambda_{m,t}), \tau_{m,t} \right\}_{m \in \mathcal{M}}, \quad (18)$$

where  $Q_{m,t} \in \mathbb{Z}_{\geq 0}$  is the queue length for movement  $m$ ,  $\lambda_{m,t} \in \mathbb{R}_{\geq 0}$  is the arrival intensity, and  $\tau_{m,t} \in \mathbb{R}_{\geq 0}$  is the service age (time since last service). Let  $y_t$  denote the latent aggregated state

$$y_t \triangleq (Q_{1,t}, \dots, Q_{M,t}, \lambda_{1,t}, \dots, \lambda_{M,t}, \tau_{1,t}, \dots, \tau_{M,t}). \quad (19)$$

The reduced belief is  $b_t(y) \triangleq p(y_t = y \mid z_{1:t}, u_{1:t-1})$  and is updated by an approximate filter of the same predict-update form as (16)–(17), but using a learned/parametric aggregated transition model  $p(y_{t+1} \mid y_t, u_t)$  and an observation likelihood  $p(z_t \mid y_t)$  (estimated via calibrated vision uncertainty).

### I. Aggregated Dynamics and Counterfactual Rollouts

For each movement  $m \in \mathcal{M}$ , the queue evolves as

$$Q_{m,t+1} = \max\left(0, Q_{m,t} + A_{m,t} - S_{m,t}(u_t)\right), \quad (20)$$

where arrivals follow a count model (e.g., Poisson)

$$A_{m,t} \sim \text{Poisson}(\lambda_{m,t} \Delta t), \quad (21)$$

and service is bounded by saturation flow  $\mu_m$ :

$$0 \leq S_{m,t}(u_t) \leq \mu_m \Delta t. \quad (22)$$

Service ages update deterministically:

$$\tau_{m,t+1} = \begin{cases} 0, & \text{if movement } m \text{ is served under action } u_t, \\ \tau_{m,t} + \Delta t, & \text{otherwise.} \end{cases} \quad (23)$$

a) *Counterfactual rollout operator*.: Given belief  $b_t$ , candidate action  $u$ , and horizon  $H$ , define the rollout distribution over future beliefs

$$\hat{b}_{t+k}^u \triangleq \text{Rollout}(b_t, u, k), \quad k = 0, \dots, H, \quad (24)$$

obtained by iterating the aggregated transition model  $p(y_{t+1} \mid y_t, u_t)$  and the filter update with synthetic observations (or equivalently, propagating the belief through the predictive model when using an open-loop horizon). In implementation,  $\hat{b}_{t+k}^u$  is represented by particles or parametric distributions over  $(Q_{m,t+k}, \lambda_{m,t+k}, \tau_{m,t+k})$ .

For compactness, we denote the sequence of predicted beliefs as

$$\hat{b}_{t:t+H}^u \triangleq \{\hat{b}_t^u, \hat{b}_{t+1}^u, \dots, \hat{b}_{t+H}^u\}. \quad (25)$$

### J. Predictive Dilemma-Zone Risk Functional (Derived)

A yellow onset is unsafe if at least one approaching vehicle is in the dilemma zone at the decision time, i.e., it cannot stop comfortably before the stop line and also cannot clear the intersection before red. For an approaching vehicle  $i$ , let  $(v_i, d_i)$  be its speed and distance-to-stopline at decision time. Under bounded deceleration  $a_{\max} > 0$  and driver reaction time  $\delta_r \geq 0$ , define:

a) *Stopping feasibility*.: The minimum stopping distance is

$$d_{\text{stop}}(v_i) \triangleq v_i \delta_r + \frac{v_i^2}{2a_{\max}}. \quad (26)$$

Stopping is feasible if  $d_i \geq d_{\text{stop}}(v_i)$ .

b) *Clearing feasibility*.: Let  $L_i$  denote the effective distance to clear (distance-to-stopline plus intersection width plus vehicle length margin). Let  $T_y$  be the yellow duration and  $T_{ar}$  the all-red clearance. Clearing is feasible if the time-to-clear satisfies

$$t_{\text{clr}}(v_i, d_i) \triangleq \frac{L_i}{\max(v_i, v_{\min})} \leq T_y + T_{ar}, \quad (27)$$

where  $v_{\min} > 0$  avoids division by zero (a conservative modeling choice).

c) *Dilemma-zone event*.: Define the dilemma event for vehicle  $i$  at yellow onset:

$$\mathcal{D}_i \triangleq (d_i < d_{\text{stop}}(v_i)) \wedge (t_{\text{clr}}(v_i, d_i) > T_y + T_{ar}). \quad (28)$$

Let  $\mathcal{I}_t$  be the set of vehicles deemed relevant (e.g., tracked vehicles in approach lanes within a lookahead distance). The overall dilemma-zone event is

$$\mathcal{D} \triangleq \bigcup_{i \in \mathcal{I}_t} \mathcal{D}_i. \quad (29)$$

*d) Belief-conditional risk.*: Under vision uncertainty,  $(v_i, d_i)$  are random variables. UCATSC models their joint uncertainty via the belief  $\hat{b}_{t+k}^u$  (through the tracking posterior and/or a calibrated kinematic error model). The predictive dilemma-zone risk for initiating yellow under candidate action  $u$  at step  $k$  is

$$\mathcal{R}_{\text{DZ}}(\hat{b}_{t+k}^u) \triangleq \mathbb{P}(\mathcal{D} \mid \hat{b}_{t+k}^u). \quad (30)$$

*e) Computable upper bound (optional).*: If independence across vehicles is assumed (conservative if violated), then

$$\mathcal{R}_{\text{DZ}}(\hat{b}_{t+k}^u) = 1 - \prod_{i \in \bar{I}_t} \left(1 - \mathbb{P}(\mathcal{D}_i \mid \hat{b}_{t+k}^u)\right). \quad (31)$$

Alternatively,  $\mathcal{R}_{\text{DZ}}$  can be estimated by Monte Carlo samples from  $\hat{b}_{t+k}^u$  (particles over kinematics), yielding an unbiased estimator.

#### K. Complete Belief-Space CS-MPC Optimization Problem

At each decision epoch  $t$ , UCATSC chooses an action  $u_t$  from a *legally admissible* set  $\mathcal{U}_{\text{adm}}(p_t)$  determined by the active phase  $p_t \in \mathcal{P}$  and intergreen rules.

*a) Decision variables.*: We optimize over a *one-step* action  $u_t \in \mathcal{U}_{\text{adm}}(p_t)$  in receding-horizon fashion, while evaluating its consequences via a horizon- $H$  rollout  $\hat{b}_{t:t+H}^{u_t}$ .

*b) Cost functional.*: Define expected delay surrogate on a belief as

$$D(b) \triangleq \sum_{m \in \mathcal{M}} \mathbb{E}_b[Q_m], \quad (32)$$

and define the rollout cost

$$J(b_t, u) \triangleq \mathbb{E} \left[ \sum_{k=0}^H \gamma^k D(\hat{b}_{t+k}^u) \right], \quad (33)$$

with discount  $\gamma \in (0, 1]$  (often  $\gamma = 1$  for short horizons).

*c) Hard constraints (fully specified).*: UCATSC enforces the following predictive constraints along the rollout:

**(C1) Phase legality and timing:** minimum green  $g_{\min}$ , maximum green  $g_{\max}$ , fixed or bounded yellow  $T_y$ , all-red  $T_{ar}$ , and conflict-free sequencing encoded by  $\mathcal{U}_{\text{adm}}(p_t)$ .

**(C2) Dilemma-zone safety at yellow onset:** for any rollout step  $k$  where action  $u$  implies initiating yellow (a phase termination),

$$\mathcal{R}_{\text{DZ}}(\hat{b}_{t+k}^u) \leq \epsilon. \quad (34)$$

**(C3) Starvation avoidance:** for all movements and all rollout steps,

$$\tau_{m,t+k} \leq \tau_{\max}, \quad \forall m \in \mathcal{M}, k = 0, \dots, H. \quad (35)$$

**(C4) Physical service bounds:** service must satisfy (22) and queue nonnegativity via (20).

*d) Optimization (receding horizon).*: The UCATSC action selection problem is

$$\begin{aligned} u_t^* \in \arg \min_{u \in \mathcal{U}_{\text{adm}}(p_t)} & J(b_t, u) \\ \text{s.t.} & (20), (23), (22) \text{ along rollout,} \\ & (34) \text{ whenever yellow is initiated,} \\ & (35). \end{aligned} \quad (36)$$

*e) Notation consistency.*: We use:  $b_t$  for belief at time  $t$ ,  $\hat{b}_{t+k}^u$  for the predicted belief at future step  $t+k$  under candidate action  $u$ , and  $\hat{b}_{t:t+H}^u$  for the full horizon sequence.

#### L. Comparing RL with UCATSC

---

#### Algorithm 1 Reinforcement Learning-Based Traffic Signal Control

---

```

1: Inputs: state  $s_t$  (queues/counts/images), policy  $\pi_\theta$ , reward
    $R(s_t, a_t)$ 
2: loop
3:   Observe  $s_t$ 
4:   Select action  $a_t \leftarrow \pi_\theta(s_t)$ 
5:   Execute  $a_t$ 
6:   Receive  $s_{t+1}$  and reward  $R(s_t, a_t)$ 
7:   Safety handled implicitly via reward shaping or action
      masking
8: end loop

```

---



---

#### Algorithm 2 UCATSC: Uncertainty-aware Counterfactual Adaptive Traffic Signal Control

---

```

1: Inputs: vision observations  $z_t$ , geometry  $\mathcal{G}$ , phase set  $\mathcal{P}$ ,
   thresholds  $\epsilon, \tau_{\max}$ , horizon  $H$ 
2: State: belief  $b_t = \{p(Q_{m,t}), p(\lambda_{m,t}), \tau_{m,t}\}_{m \in \mathcal{M}}$ 
3: loop
4:   Observe  $z_t$ 
5:   Update belief  $b_t \leftarrow p(b_t \mid z_t)$   $\triangleright$  explicit uncertainty
   update
6:   Generate admissible actions  $\mathcal{A} \subseteq \mathcal{U}$ 
7:   for all  $a \in \mathcal{A}$  do
8:     Rollout future beliefs  $\hat{b}_{t:t+H}^a$  using  $\mathcal{T}$ 
9:     Check safety:  $\mathcal{R}_{\text{DZ}}(\hat{b}_{t+k}^a) \leq \epsilon$ 
10:    Check starvation:  $\tau_{m,t+k} \leq \tau_{\max}$  for all  $m$ 
11:    Compute expected cost  $J(a)$  via (5)
12:   end for
13:   Select  $a^* = \arg \min_{a \in \mathcal{A}} J(a)$  subject to constraints
14:   Execute  $a^*$ 
15: end loop

```

---

#### M. Assumptions, Formal Conditions, and Online Validity Checks

UCATSC operates under boundedness and local-stationarity assumptions that define its operational design domain and make belief-space optimization tractable. When violated, the controller should degrade to conservative fallback timing.

**A1 (Bounded perception error).** Let the vision pipeline produce aggregated features  $\hat{s}_t$  from  $z_t$ . Assume an error envelope over the short horizon:

$$\|s_t - \hat{s}_t\| \leq \delta_s \quad \text{with probability } \geq 1 - \eta. \quad (37)$$

UCATSC uses  $(\delta_s, \eta)$  to inflate uncertainty in belief update and risk evaluation.

**A2 (Known geometry and conflict graph).** The phase set  $\mathcal{P}$  and conflict graph  $\mathcal{G}$  are fixed.

**A3 (Local stationarity of arrivals).** For each movement  $m$ :

$$|\lambda_{m,t+k} - \lambda_{m,t}| \leq L_\lambda k \Delta t, \quad k = 0, \dots, H. \quad (38)$$

**A4 (Bounded service and saturation stability).** With saturation flow  $\mu_m$ :

$$0 \leq S_{m,t}(u_t) \leq \mu_m \Delta t, \quad (39)$$

$$|S_{m,t+1} - S_{m,t}| \leq L_S. \quad (40)$$

**A5 (Finite horizon sufficiency).** Decisions are dominated by near-term outcomes under receding-horizon control.

**A6 (No persistent spillback within horizon).** For each movement  $m$ :

$$\mathbb{P}(\text{spillback blocks discharge of } m \text{ within } H) \leq \rho. \quad (41)$$

#### IV. EXPERIMENTS

This section reports the evaluation of UCATSC under vision uncertainty, including datasets and scenarios, baselines and ablations, metrics, results, runtime, and observed failure modes. The emphasis is on robustness, safety, and efficiency tradeoffs when control decisions must be made from imperfect visual information.

##### A. Datasets and Scenarios

A small-scale intersection model provides visual sensor data for evaluating UCATSC, which results in a total of 8.75 hours of data captured. From one fixed top-down camera angle, three distinct crossing configurations were monitored. Video was captured at 30 frames per second with a quality of 1080p.

The traffic demand profiles simulated vary from low to high density, with arrival-rate distributions between 1 and 5 vehicles per minute and mixed turning proportions  $[p_{\text{left}}, p_{\text{through}}, p_{\text{right}}]$ . Light shifts between daytime and nighttime form part of the setting, while planned obstructions mimic real-world camera interference. Instead of relying on full views, systems respond to varying illumination levels from low to very high, or partially blocked lenses. Vehicle detections and tracks are produced by a vision pipeline that outputs per-movement observations, including presence, motion state, and detection confidence.

To explicitly stress-test robustness under perception uncertainty, the evaluation is structured into multiple scenario classes:

- **S1:** One type involves clear views and regular activity levels.
- **S2:** Obstructions appear now and then in another, due to objects partly blocking sight or repeated crossings.
- **S3:** In more intense cases, long stretches of blocked vision or constant overlapping movement occur.
- **S4:** Traffic that stays close to maximum capacity forms a separate category.
- **S5:** When possible, scenarios also mix in irregular human-like crossings among vehicles.

Each situation uses episodes with a fixed horizon of  $T$  seconds with  $R$  randomized trials. All runs log per-step belief estimates, selected actions, and proxy metrics.

##### B. Baselines and Ablations

UCATSC is compared against several baseline control strategies:

- **Fixed-time control:** Fixed-time control operates on a static schedule - green times stay unchanged, with no real-time adaptation.
- **Occupancy-based control:** Occupancy-based methods adjust using sensor triggers when vehicles cross detection zones, reacting to threshold breaches instead of flow patterns.
- **Queue-based (queue-proxy) policy:** A queue-based (queue-proxy) policy that prioritizes movements with the largest instantaneous queue proxy signal.
- **Full UCATSC:** Performance is also reported for the full UCATSC system, which employs belief-space constrained MPC with counterfactual rollouts, safety constraints, and starvation avoidance.

To isolate the contribution of individual UCATSC components, ablation studies are conducted:

- **No EMA / smoothing:** Removes temporal smoothing.
- **No hold constraint:** Disables phase-stability and minimum-hold logic.
- **No motion belief:** Removes motion-level belief aggregation from the state representation.

##### C. Metrics

Although performance assessment relies on proxy metrics derived straight from the vision system, the following measures are used:

- **Queue proxy** ( $\text{sum } QZ\_countw$ ): Calculated by adding up weighted queue signals, closely tied to delays.
- **Stopped-vehicle proxy** ( $\text{sum } QZ\_stoppedw$ ): Tracks halted vehicles, revealing stop-and-go patterns along with idling losses.
- **Risk proxy:** Approximates potential conflicts during light changes.
- **Occlusion proxy** ( $1 - p_{\text{det}}$ ): Shows how often objects go unnoticed.
- **Runtime (ms):** Captures processing time per control step.

Emission-linked indicators are computed by integrating queue, stopped-vehicle, and risk-spike signals over time to obtain idle, queue, risk-spike, and total emission proxies.

##### D. Results and Analysis

TABLE I: Mean occlusion proxy ( $1 - p_{\text{det}}$ ) with 95% confidence intervals across controllers. Green “+” indicates improvement and red “-” indicates degradation relative to the queue-based controller.

Controller	Occlusion Proxy (mean $\pm$ 95% CI)
Queue-based (queue proxy)	0.03545 [0.03476, 0.03614]
UCATSC (full)	+3.0% 0.03438 [0.03092, 0.03783]
No EMA	+0.1% 0.03540 [0.03451, 0.03629]
No Hold	+5.8% 0.03339 [0.02875, 0.03803]
No Motion	+6.0% 0.03332 [0.03028, 0.03637]

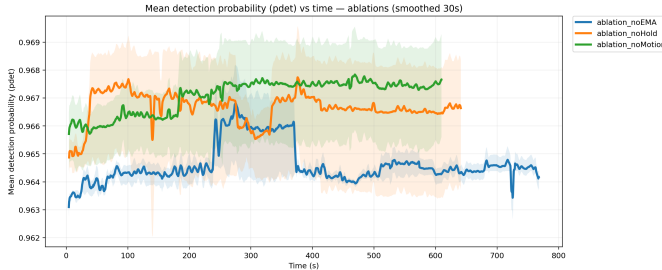


Fig. 2: Mean detection probability  $p_{\text{det}}$  vs. time (baselines, 30 s smoothing). UCATSC maintains higher and more stable detection confidence during vision degradation.

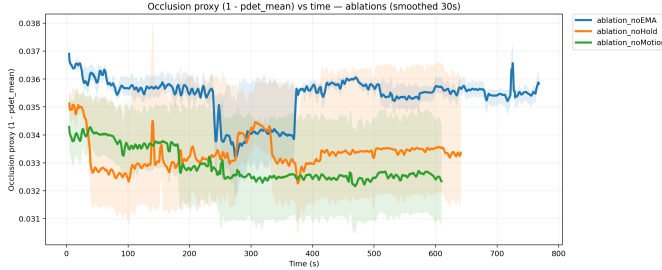


Fig. 3: Occlusion proxy ( $1 - p_{\text{det}}$ ) vs. time (baselines, 30 s smoothing). UCATSC suppresses worst-case occlusion spikes relative to fixed-time control.

a) *Robustness under occlusion (primary result).*: Results demonstrate that UCATSC is significantly more robust under occlusion compared to fixed-time control. During sustained vision degradation intervals, fixed-time control exhibits pronounced occlusion spikes, whereas UCATSC remains substantially more stable. The worst-case occlusion proxy reaches approximately 0.046 under fixed-time control but only about 0.036 under UCATSC, corresponding to a 21% reduction in peak occlusion severity. Furthermore, the mean occlusion proxy is reduced by 9.2% relative to fixed-time control and by 4.2% relative to occupancy-based control, highlighting the effectiveness of uncertainty-aware belief-space reasoning in maintaining stable operation under degraded sensing conditions.

b) *Safety behavior (risk proxy).*: Median risk proxy values are comparable across methods; UCATSC consistently eliminates extreme tail behavior. Queue-based control has the most significant high-risk excursions, while UCATSC minimizes transient risk spikes.

c) *Queueing and stop–go behavior.*: Queue proxy distribution appears similar across approaches in the scenario window, suggesting that UCATSC does not impose additional congestion. However, the stopped-vehicle proxy time series shows that aggressive adaptive approaches have significant stop-and-go oscillations, while UCATSC maintains a more stable service with degraded sensing.

d) *Emissions and energy proxies.*: As compared with the queue controller, significant reductions have been made in all directions: **48%** reduction in idle proxy, **40%** reduction in queue proxy, and **44%** reduction in risk-spike proxy. Overall, this entails a **43% reduction in total emission proxy**. Compared

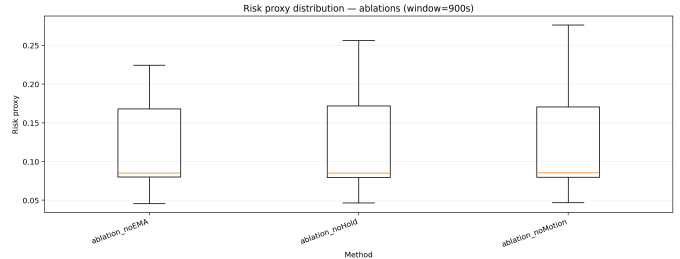


Fig. 4: Risk proxy distribution across baselines (900 s window). UCATSC reduces extreme tail risk while maintaining a comparable median.

with occupancy control, steady yet modest improvements have been made by the UCATSC algorithm (approximately **3–10%**). Compared with fixed-time control, the total emission proxy for the former is slightly lower (approximately **5–8%**) in this experimental configuration, reflecting the stability associated with steady demand.

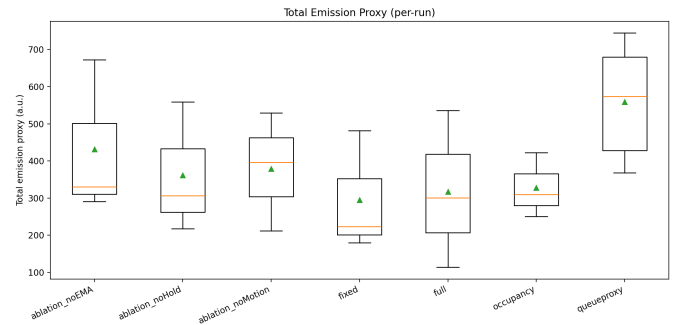


Fig. 5: Total emission proxy distribution across baselines (per-run). UCATSC achieves substantially lower emissions than queue-based control.

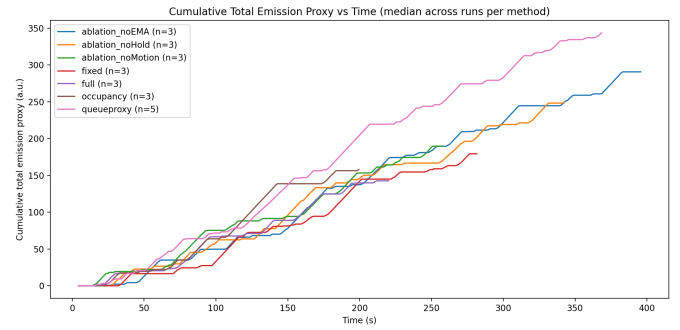


Fig. 6: Median cumulative total emission proxy vs. time. UCATSC accumulates emission cost substantially more slowly than queue-based control.

e) *Why UCATSC does not outperform fixed-time in emissions.*: UCATSC is not designed solely to minimize emissions alone. Unlike fixed-time control, UCATSC explicitly enforces safety constraints, fairness, and starvation avoidance. These mechanisms intentionally prevent overly long greens and excessive prioritization of dominant approaches, even when

TABLE II: Emission proxy means with 95% confidence intervals (per run). Green “+” denotes reduction (improvement) and red “-” denotes increase relative to the queue-based controller.

Controller	Idle Proxy	Queue Proxy	Risk Proxy	Total Emission Proxy
Queue-based	226.31 [145.30, 307.31] +51.3%	313.85 [201.29, 426.41] +44.3%	18.77 [12.49, 25.05] +49.0%	558.93 [359.96, 757.91] +47.3%
Fixed-time	110.27 [-47.60, 268.15] +42.1%	174.68 [-59.65, 409.00] +40.9%	9.57 [-3.64, 22.79] +42.6%	294.53 [-110.61, 699.66] +41.5%
Occupancy-based	131.00 [41.27, 220.72] +47.7%	185.53 [59.72, 311.33] +40.2%	10.78 [1.41, 20.14] +43.6%	327.30 [110.71, 543.88] +43.4%
UCATSC (full)	118.45 [-91.20, 328.10]	187.61 [-112.08, 487.30]	10.58 [-5.83, 26.99]	316.63 [-209.03, 842.30]

doing so would marginally reduce idle time.

*f) Runtime and deployability.*: Controller runtime stabilizes after a brief warm-up, with per-step latency near 110–120 ms, supporting real-time feasibility.

## V. DISCUSSION

### A. Overall performance trends

Despite fluctuations across tested scenarios, UCATSC shows steadier performance compared to fixed-time and actuated methods. Notably, queue lengths and risk indicators display less spread - suggesting reduced outliers during decision-making under imperfect visual data. which means there are fewer extreme values when making control decisions with partial/noisy camera observations.

### B. Impact of uncertainty-aware control

The biggest gaps in performance appear when vision uncertainty is moderate or high. In these cases, baseline controllers overreact to fleeting detection errors. By explicitly modeling uncertainty in what we observe, UCATSC prevents unnecessary phase shifts and provides more consistent phase timing. Consistency improves robustness as well as overall efficiency.

### C. Safety-related outcomes

Although rare, shifts in signal timing can trigger serious consequences - UCATSC reduces how often these extreme outcomes appear by trimming the outer edges of risk estimates. Because once a light switches, there is no going back, limiting those high-impact tails matters greatly.

### D. Interpretability of observed behavior

Because UCATSC uses organized rules to guide decisions, the gains in performance link directly to specific controls rather than unclear patterns from policy training. It becomes simpler to spot when things go wrong, which strengthens trust in the outcomes observed.

### ACKNOWLEDGMENTS

This work was fully implemented by the authors, including the modeling, control logic, experimental design, data collection, and analysis.

The authors gratefully acknowledges the Python open-source ecosystem and the developers of libraries that supported this research, including NumPy, Pandas, SciPy, Matplotlib, OpenCV, and the Ultralytics YOLO framework. These tools were used

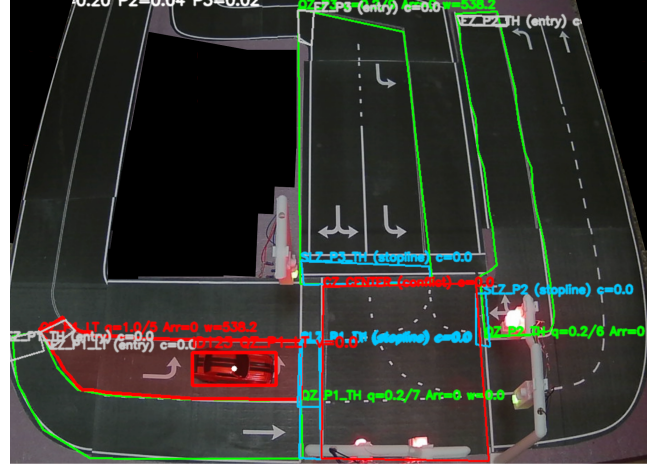


Fig. 7: **Vision-based perception and zone-level state abstraction in the UCATSC testbed.** A snapshot of the physical intersection as seen by the fixed overhead camera is provided, showing where vehicles are with detections superimposed over the actual intersection map. Vehicle detections are then aggregated into three types of zones: Queue Zones (QZ), Stop-Line Zones (SLZ), and a shared Conflict Zone (CZ). Zone level state is then used to create proxies for queue length, queue occupancy, and risk. This is the only state that is fed into the UCATSC controller.

solely as supporting infrastructure for numerical computation, computer vision, and visualization.

The authors also thanks the broader open-source community for making robust and well-documented software resources publicly available.

### REFERENCES

- [1] M. Papageorgiou, C. Diakaki, V. Dinopoulou, A. Kotsialos, and Y. Wang, “Review of road traffic control strategies,” *Proceedings of the IEEE*, vol. 91, no. 12, pp. 2043–2067, 2003.
- [2] M. Barth and K. Boriboonsomsin, “Traffic congestion and greenhouse gases,” *ACCESS Magazine*, no. 35, pp. 2–9, 2009.
- [3] H. Rakha and K. Ahn, “Integration modeling framework for estimating mobile source emissions,” *Journal of Transportation Engineering*, vol. 130, no. 2, pp. 183–193, 2004.
- [4] Y. Zhang, M. Barth, and K. Boriboonsomsin, “Emission impacts of traffic signal control strategies: Field evaluation,” *Transportation Research Part D: Transport and Environment*, vol. 16, no. 4, pp. 296–303, 2011.
- [5] J. Fan *et al.*, “Analyzing the emission impact of signal control on mixed traffic flow,” *Sustainability*, vol. 15, no. 22, 2023.
- [6] C. Yu *et al.*, “A systematic review of urban road traffic co<sub>2</sub> emissions,” *Carbon Footprint*, vol. 4, no. 1, 2025.

[7] U.S. Environmental Protection Agency, "Emission facts: Idling vehicle emissions," U.S. EPA, Tech. Rep. EPA-420-F-08-025, 2008.

[8] World Health Organization, "Health effects of particulate matter," WHO Regional Office for Europe, Tech. Rep., 2013.

[9] J. Lelieveld, J. S. Evans, M. Fnais, D. Giannadaki, and A. Pozzer, "The contribution of outdoor air pollution sources to premature mortality," *Nature*, vol. 525, pp. 367–371, 2015.

[10] J. Ma, X. Hu, and M. Barth, "Green traffic signal control for reducing vehicle emissions," *IEEE Transactions on Intelligent Transportation Systems*, vol. 21, no. 3, pp. 1257–1268, 2020.

[11] K. Dresner and P. Stone, "A multiagent approach to autonomous intersection management," *Journal of Artificial Intelligence Research*, vol. 31, pp. 591–656, 2008.

[12] H. Wei, C. Chen, G. Zheng, K. Wu, V. Gayah, K. Xu, and Z. Li, "Presslight: Learning max pressure control to coordinate traffic signals in arterial networks," in *Proceedings of the 25th ACM SIGKDD International Conference on Knowledge Discovery and Data Mining*, 2019, pp. 1290–1298.

[13] E. van der Pol and F. A. Oliehoek, "Coordinated deep reinforcement learners for traffic light control," in *NeurIPS Workshop on Deep Reinforcement Learning*, 2016.

[14] L. Li *et al.*, "Traffic signal timing via deep reinforcement learning," *IEEE/CAA Journal of Automatica Sinica*, vol. 3, no. 3, pp. 247–254, 2016.

[15] S. Sivaraman and M. Trivedi, "Looking at vehicles on the road," *IEEE Transactions on Intelligent Transportation Systems*, vol. 14, no. 4, pp. 1773–1795, 2013.

[16] J. Azimjonov and A. M. Ozbayoglu, "Real-time vehicle detection and tracking for vision-based traffic monitoring," *Sensors*, vol. 18, no. 11, 2018.

[17] H. Zeng *et al.*, "Learning traffic signal control from raw images," in *Proceedings of the AAAI Conference on Artificial Intelligence*, 2020.

[18] A. Müller and M. Sabatelli, "Safe and psychologically pleasant traffic signal control with reinforcement learning using action masking," *arXiv preprint arXiv:2206.10122*, 2022. [Online]. Available: <https://arxiv.org/abs/2206.10122>

[19] R. Zhou *et al.*, "Constrained reinforcement learning for traffic signal control," *Expert Systems with Applications*, vol. 239, 2024.

[20] C. Liu, R. Herman, and D. Gazis, "A review of the yellow interval dilemma," *Transportation Research Part A: Policy and Practice*, vol. 30, no. 5, pp. 333–348, 1996.

[21] N. Elmitiny *et al.*, "Red light running violations and crash risk at signalized intersections," *Accident Analysis and Prevention*, vol. 42, no. 1, pp. 159–167, 2010.

[22] J. Bonneson, *Engineering Analysis of Signalized Intersections*. McGraw-Hill, 2011.

[23] J. Ault, J. P. Hanna, and G. Sharon, "Learning an interpretable traffic signal control policy," in *Proceedings of the International Conference on Autonomous Agents and Multiagent Systems*, 2020.

[24] F. Belletti *et al.*, "Expert-level control of traffic signals," *Nature*, vol. 604, pp. 236–241, 2022.

[25] Federal Highway Administration, "Traffic signal timing manual," FHWA, Tech. Rep. FHWA-HOP-08-024, 2008.

[26] N. Gartner, C. Messer, and A. Rathi, *Traffic Flow Theory: A State-of-the-Art Report*. FHWA, 2001.

[27] H. Rakha, K. Ahn, and A. Trani, "Development of vt-micro model for estimating hot stabilized light duty vehicle and truck emissions," *Transportation Research Part D*, vol. 9, no. 1, pp. 49–74, 2004.

[28] M. Barth and K. Boriboonsomsin, "Real-world carbon dioxide impacts of traffic congestion," *Transportation Research Record*, vol. 2058, pp. 163–171, 2008.

[29] A. A. Karner, D. S. Eisinger, and D. A. Niemeier, "Near-roadway air quality: Synthesizing the findings from real-world data," *Environmental Science & Technology*, vol. 44, no. 14, pp. 5334–5344, 2010.

[30] A. Stevanovic, "Adaptive traffic control systems: Domestic and foreign state of practice," FHWA, Tech. Rep., 2010.

[31] P. Mirchandani and K. Head, "A review of traffic signal control methods," Tech. Rep., 2001.

[32] D. I. Robertson, "Transyt: A traffic network study tool," *Traffic Engineering & Control*, 1969.

[33] N. Gartner, "Opac: A demand-responsive strategy for traffic signal control," *Transportation Research Record*, 1983.

[34] B. Coifman, "Vehicle reidentification and travel time measurement using loop detector signatures," *Transportation Research Part C*, vol. 6, no. 6, pp. 371–388, 1998.

[35] Z. Sun, G. Bebis, and R. Miller, "On-road vehicle detection: A review," *IEEE Transactions on Pattern Analysis and Machine Intelligence*, vol. 28, no. 5, pp. 694–711, 2006.

[36] P. Varaiya, "Max pressure control of a network of signalized intersections," *Transportation Research Part C*, vol. 36, pp. 177–195, 2013.

[37] P. B. Hunt, D. I. Robertson, R. D. Bretherton, and R. I. Winton, "Scoot—a traffic responsive method of coordinating signals," TRL, Tech. Rep., 1981.

[38] P. R. Lowrie, "Scats: The sydney coordinated adaptive traffic system," in *International Conference on Road Traffic Signalling*, 1982.

[39] P. Mirchandani and K. Head, "A real-time traffic signal control system: Architecture, algorithms, and analysis," *Transportation Research Part C*, vol. 9, no. 6, pp. 415–432, 2001.

[40] P. Dollar, C. Wojek, B. Schiele, and P. Perona, "Pedestrian detection: An evaluation of the state of the art," *IEEE Transactions on Pattern Analysis and Machine Intelligence*, vol. 34, no. 4, pp. 743–761, 2012.

[41] D. Amodei *et al.*, "Concrete problems in ai safety," *arXiv preprint arXiv:1606.06565*, 2016.

[42] A. Y. Ng, D. Harada, and S. Russell, "Policy invariance under reward transformations: Theory and application to reward shaping," in *ICML*, 1999.

[43] F. Doshi-Velez and B. Kim, "Towards a rigorous science of interpretable machine learning," *arXiv preprint arXiv:1702.08608*, 2017.

[44] F. V. Webster, "Traffic signal settings," Road Research Laboratory, Tech. Rep., 1958.

[45] V. Kastrinaki, M. Zervakis, and K. Kalaitzakis, "A survey of video processing techniques for traffic applications," *Image and Vision Computing*, vol. 21, no. 4, pp. 359–381, 2003.

[46] L. P. Kaelbling, M. L. Littman, and A. R. Cassandra, "Planning and acting in partially observable stochastic domains," *Artificial Intelligence*, vol. 101, no. 1, pp. 99–134, 1998.

[47] D. Gazis, R. Herman, and A. Maradudin, "The problem of the amber signal light in traffic flow," *Operations Research*, vol. 8, no. 1, pp. 112–132, 1960.

[48] J. W. S. Liu, *Real-Time Systems*. Prentice Hall, 2000.

[49] C. Papadimitriou and J. Tsitsiklis, "The complexity of markov decision processes," *Mathematics of Operations Research*, vol. 12, no. 3, pp. 441–450, 1987.

[50] S. Thrun, W. Burgard, and D. Fox, *Probabilistic Robotics*. MIT Press, 2005.

[51] G. Williams *et al.*, "Information-theoretic mpc for model-based reinforcement learning," in *ICRA*, 2017.

[52] X. Li *et al.*, "Urban traffic video datasets: A survey," *IEEE Intelligent Transportation Systems Magazine*, 2020.

[53] M. Li, C. Liu, Z. Li, X. Liu, G. Yu, B. Du, J. Shen, and Q. Wu, "Cflight: Enhancing safety with traffic signal control through counterfactual learning," 2025. [Online]. Available: <https://arxiv.org/abs/2512.09368>